

11th CIRP Conference on Photonic Technologies [LANE 2020] on September 7-10, 2020

LMD coatings as filler material for laser beam welded 30 mm thick plates

Anne StraÙe^{a*}, Ömer Üstündağ^a, Andrey Gumenyuk^a, Michael Rethmeier^{b, a}

^aBundesanstalt für Materialforschung und -prüfung (BAM), Unter den Eichen 87, 12205 Berlin, Germany

^bTechnische Universität Berlin, Pascalstraße 8-9, 10587 Berlin, Germany

* Corresponding author. Tel.: +49 30 8104 4864; E-mail address: anne.strasse@bam.de

Abstract

The development of high energy laser sources enables single-pass welds of thick plates up to 30 mm, but often additional materials are needed to influence the properties of the weld seams. However, the homogenous distribution of filler materials in form of e.g. electrodes is only possible up to 7 mm while the elements are only traceable up to a depth of 14 mm. To overcome this problem a two-step process is used where first the edges of the weld partners are coated with the filler material by laser metal deposition (LMD) and afterwards are welded by laser beam. Single-pass welds with electromagnetic weld pool support of 30 mm thick S355 J2+N-plates with austenitic AISI 316L-coatings were investigated as well as the influence of the coatings to the penetration depth of the laser beam without electromagnetic weld pool support in double-sided joints. The weld seams were tested by X-ray inspection and cross sections.

© 2020 The Authors. Published by Elsevier B.V.

This is an open access article under the CC BY-NC-ND license (<http://creativecommons.org/licenses/by-nc-nd/4.0/>)

Peer-review under responsibility of the Bayerisches Laserzentrum GmbH

Keywords: Laser Metal Deposition (LMD); laser beam welding; filler material distribution; penetration depth

1. Introduction

The development of high energy laser sources opens the market for new applications due to the fact, that plates with higher thicknesses are weldable in a single pass. The advantages of the laser like a low heat input, a high welding speed combined with little distortion are obvious. However, there are two challenges to overcome with this technique and its application for thick plates. The first one relates to a process instability at slower welding velocity, which is required to achieve a full penetration welding with an increasing plates thickness at the limited laser power. This results in a higher volume of molten material and thus a competition of the hydrostatic pressure p_h which is dependent on the plate thickness h with Laplace pressure p_L , which in turn is dependent on the surface tension. If the Laplace pressure cannot compensate the hydrostatic pressure, this results in drop-out on the root side often in combination with melt sagging on the upper side [1]. Common approaches are melt pool support systems or multi-layer welds. Both are time consuming due to

necessary preparations, rework or the higher process times.

Nomenclature

B	Magnetic field in T
F_L	Lorentz force in N
f	Defocussing in mm
f_{AC}	AC-Magnet frequency in Hz
h	Plate thickness in mm
HAZ	Heat affected zone
H LAW	Hybrid laser-arc welding
j	Electric current density in $A \cdot m^{-2}$
LB	Laser beam
LMD	Laser metal deposition
P_{AC}	AC-Magnet power in kW
P_L	Laser power in kW
p_h	Hydrostatic pressure in Pa
p_L	Laplace pressure in Pa
v_s	Welding speed in $m \cdot min^{-1}$

Another, third approach is a non-contact weld pool support system based on electromagnetic compensation of the hydrostatic pressure. It was developed and investigated by Avilov et al. [1] for high power laser welds and further investigated by other authors for the hybrid laser-arc welding (HLAW) process [2]. This compensation works by utilization of an AC-magnet system, which is placed below the specimen and generates an oscillating magnetic field B perpendicular to the welding direction, that in turn induces the electric current density j parallel to the welding direction. The resulting Lorentz force F_L is directed upwards, contrary to the hydrostatic pressure.

The second challenge, which works as a limiting factor at the higher plate thickness is the dilution of the molten material. Many applications need filler materials to influence the weld seam to a certain purpose. A prominent example for this is the usage of filler materials with a higher nickel content for duplex stainless steels laser welding to achieve a higher austenite fraction [3, 4]. Gook et al. [5] showed, that the maximum depth in which the elements of the filler material could be detected is 14 mm and that the distribution through the depth of the weld is uneven for laser hybrid welds, as shown in Fig. 1.

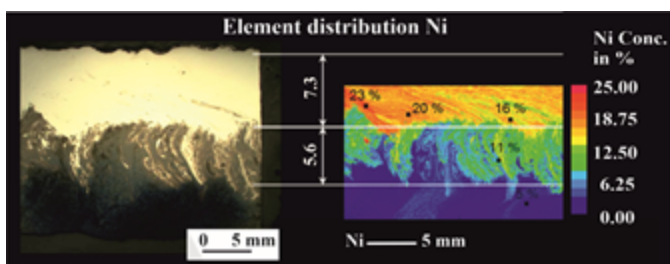


Fig. 1 Element distribution of Ni in length section of laser hybrid welded seam [6]

To overcome this problem different approaches like multi-layer welds with a filler wire or the usage of nickel foils, that were placed between the weld partners were used [3, 7]. For 15 mm thick duplex plates a two-step process was proposed by StraÙe et al. [8], were in the first step the filler material was deposited on the weld partners by laser metal deposition (LMD) and those coated edges were welded by laser beam (LB) afterwards. In this paper two approaches for 30 mm butt joints, single-pass with electromagnetic weld pool support and double-sided joints without the magnetic system are investigated and compared. For both the above described welds a prior coating process by LMD was used.

2. Experimental setup

The base material was a S355 J2+N structural steel with the dimensions of 100 mm x 300 mm x 30 mm. As filler material an AISI 316L-Si austenitic stainless-steel powder with the particle size of 53 μm - 106 μm was used. This material combination has no practical applications. It was chosen, because of the good distinguishability of both phases in microsections and thus to show the effects of both welding approaches. For both materials the chemical composition according to the manufacturers specifications is shown in Table 1.

Table 1. Chemical composition (wt.-%) of the materials

Elements	S355 J2+N (wt.-%)	AISI 316L-Si (wt.-%)
C	0.15	0.01
Si	0.19	2.1
Mn	1.55	0.4
P	0.012	0.01
S	0.003	-
Cr	0.009	17.3
Mo	-	2.5
Ni	-	12.2
Fe	Bal.	Bal.

The coating of the edges was done by LMD with a five-axis Trumpf TruLaser Cell 3000 working station, which is equipped with a 16 kW Trumpf TruDisc 16002 Yb:YAG-disc laser with the wave length of 1030 nm. For the powder distribution a Medicoat Flowmotion Twin powder feeder was used with a powder feed rate of 17 $\text{m}\cdot\text{min}^{-1}$.

The coaxial three-jet nozzle has a working distance of 16 mm with a powder spot diameter of approx. 3.5 mm and the chosen parameters were a laser spot diameter of 2.4 mm, a welding velocity of 1.3 $\text{m}\cdot\text{min}^{-1}$ and a laser power of 1.2 kW. The coating of the edges has been made as a single layer with 21 overlapping tracks with a track width of approx. 2.9 mm and a stepover of 1.38 mm.

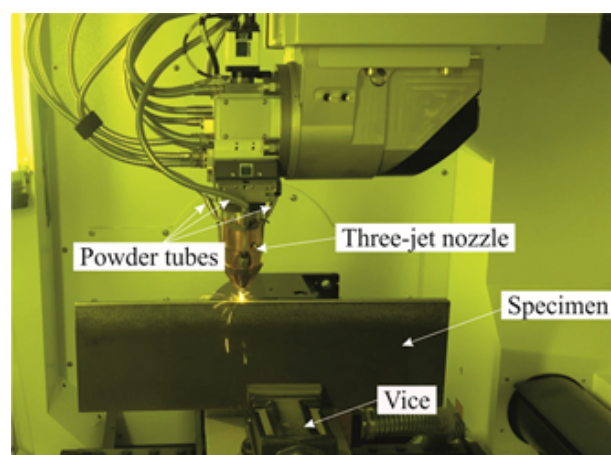


Fig. 2 Experimental setup for the edge coating by LMD

For the laser welding an IPG YLR-20000 fiber laser with a wavelength of 1070 nm, a focus diameter of 0.56 mm and a beam parameter product of 11 $\text{mm}\cdot\text{mrad}$ was used.

The HIGHYAG BIMO HP-Laser processing head with a focal length of 350 mm was mounted on a 6-axis Kuka-robot. The shielding gas (argon) was delivered through a lateral shielding gas nozzle. The experimental setups for the coating and the laser welding are shown in Fig. 2 and Fig. 3, respectively.

For the single-pass welds the AC-magnetic system was installed additionally, with the specimen fixed 2 mm above the magnet poles. Here, instead of the robot with the optical head, the specimen are fixed on a linear axis is moved over the magnetic system.

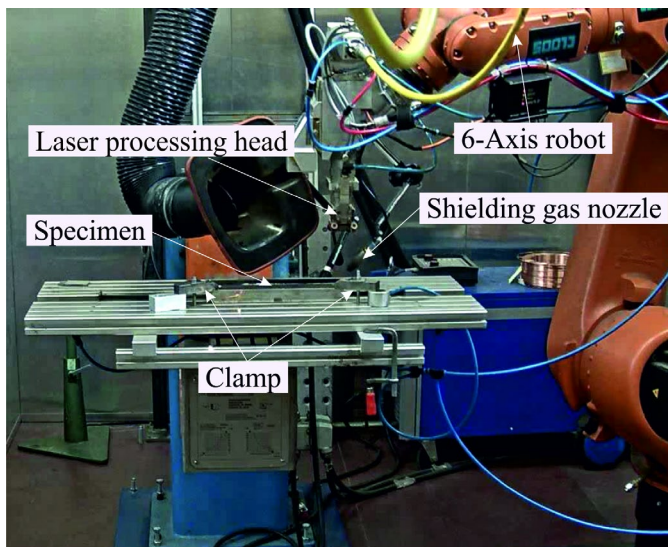


Fig. 3 Experimental setup for the laser welding of the double-sided joints

All weld seams double-sided as well as single-pass were done as butt joints in 1G-position. The welding parameters are listed in Table 2.

Table 2. Welding and AC-magnet parameters

	Single pass welds	Double-sided joints	
		Seam weld	Root weld
Welding speed v_s in $m \cdot min^{-1}$:	0.5	1.6	1.2
Laser power P_L in kW:	18.8	15.6	8.0
Defocussing f in mm:	- 8	- 4	- 4
Magnet power P_{AC} in kW:	2.4	-	-
Frequency f_{AC} in Hz:	1200	-	-

3. Results and discussion

3.1. Edge coating

The outer appearance of the deposition layer of the edges does not perform any obvious oxidation and looks homogenous.

The cross sections display a low dilution ($< 20\%$) between base material and the filler material, whereas the dilution is defined as the ratio of the volume of the coating material to the volume of the whole molten material and can be deduced from the corresponding areas in the cross sections. Fig. 4 shows a part of the cross section. It is visible, that the upper side is even. The separation between the single tracks is only possible to be recognized by the waviness of the lower section of the coating.



Fig. 4 Cross section of buttered edge

Both mentioned characteristics of the deposited layer, the even upper side as well as the low dilution, are advantageous. The edge evenness is a necessary condition for the following laser welding process for which a technical zero gap is preferred. The thickness of the coating is approx. 0.5 mm and thus sufficient to produce a laser weld within the coated material. In combination with the low dilution, this enables defined weld properties due to a known composition of the filler material, as well as a good connectivity between the base metal and the coating.

3.2. Double-sided joints

The two passes of the double-sided joints showed a good outer appearance with no visible defects. For both passes cross sections were made, to allow an inside impression of the weld's quality (cf. Fig. 5). Those showed solidification cracks and pores for both layers. The formation of hot cracks was investigated by different authors [9-11] and is influenced by a combination of the alloy composition and the welding conditions. The counter pass was done as a partial penetration weld and due to the high cooling rates typical for laser welding the degassing was hindered, which also results in pores and is a known problem for this type of weld seams [12]. Additionally, due to their crystal lattice and thus a lower dissolving ability for low melting elements austenitic stainless steels have a higher susceptibility for hot cracks than mild steels, so cracks were to be expected, but they were not under investigation and thus no efforts were made to prevent them [13].

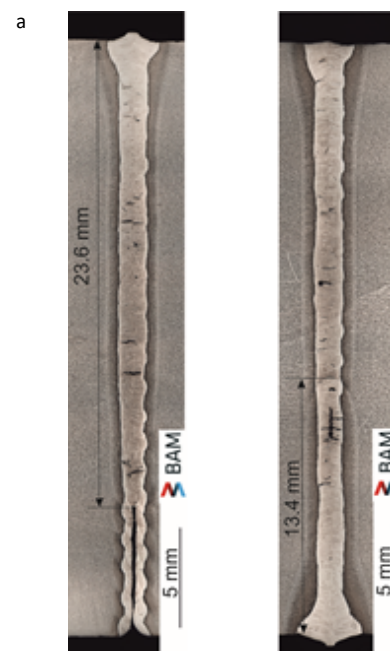


Fig. 5 Cross sections of double-sided joints (a) after the first pass; (b) after the counter pass

Unexpected was the high penetration depth of the first pass. Initially, a welding depth of slightly over half of the material thickness was aspired. With 23.6 mm for the coated edges this value was far higher than expected (< 20 mm [14]) and more than three quarters of the material thickness. This condition can

be explained with the geometry of the coatings. Even though they were quite even, due to the overlapping between single tracks a slight waviness was still evident and thus a wider gap between the valleys of coatings, which allowed for an unhindered passage of the laser beam. The influence of the edge roughness on the penetration depth was also investigated by Sokolov et al. [15] and they confirmed, that a certain roughness as well as a slight increase of the air gap have a positive influence on the penetration depth as well as the weld quality.

This was the reason for an adjustment of the welding parameters to a significant reduction of the laser power for the counter pass. Still the penetration depth was 13.4 mm which resulted in the overlap of approx. 7 mm.

With its slim shape the appearance of the weld seam is typical for laser welds. The low heat input as well as the welding speed allow for only a small volume of molten material. The waviness of the fusion line at the transition to the heat affected zone (HAZ) indicates, that the laser beam only reached the coated areas, as intended to realize known properties in the weld seam, as discussed above.

3.3. Single-pass welds with electromagnetic weld pool support

The single-pass welds also showed a good outer appearance without any visible defects. The cross section is depicted in Fig. 6 and indicates a well-formed weld seam without visible defects apart from a small pore. According to EN ISO 131919-01 the root quality is sorted to the highest evaluation group B.



Fig. 6. Cross section of single-pass weld

The x-ray analysis of the weld seams confirmed that no defects except in the starting and ending region were detected. Those areas are known for defects due a stabilization phase in the beginning and the collapse of the keyhole in the end. Usually this problem is solved by the usage of run-on or run-

off tabs, respectively. Fig.7 shows the x-ray images with the defects highlighted by black circles.

In comparison to the double-sided joints the single-pass welds are wider, with no rest coatings visible. Also, the heat affected zone appears more prominent. This increase of volume of the molten material and the HAZ was to a small part due to the higher laser power of 18.8 kW, but the main reason was the far lower welding speed of $0.5 \text{ m} \cdot \text{min}^{-1}$. Without the electromagnetic support systems such low velocities would result in dropouts in the root region.



Fig. 7. X-ray image of a single-pass weld seam with defects (black circled)

The wider weld seam resulted in a melting of not only the coating but the base material as well. This leads to a change in the composition of the weld seam alloy and thus in a probable change of the properties. To avoid this there are two possible solutions: For one the application of thicker LMD coatings with changed parameters or multiple layers. Another solution is an adjusted element distribution in the powder composition, that reacts to the changed volume of molten material and thus results in the initial aspired properties of the weld seam.

4. Conclusions

The presented two-step process, where the filler material is deposited to the edges of the weld partners by LMD in the first step, prior to the laser beam process as a second step, is a solution to realize a homogenous distribution of the filler material in the weld seam for thick plates.

The double-sided joints showed slim weld seams with a rest coating visible and thus a known element distribution in the molten material but having imperfections like hot cracks and pores.

The single-pass welds with electromagnetic weld pool support allowed for a slower welding velocity. Except for the starting and ending regions, those weld seams were defect free. The weld seams as well as the HAZ were wider due to the higher heat input and all the coating was molten as well as parts of the base material. As a result, the element distribution changed. The knowledge of the geometry and volume of the weld seams enables to adapt the coatings element composition and thus realize the aspired properties in the weld seam. Alternatively, thicker coatings realize the same goal.

Acknowledgements

This work was supported by the Federation of Industrial Research Association (AiF, project number 19.228N) and the German Federal Ministry for Economic Affairs and Energy (BMWi- Bundesministerium für Wirtschaft und Energie) based on a resolution of the Deutscher Bundestag.

References

- [1] V. Avilov, A. Gumenyuk, M. Lammers, and M. Rethmeier, "PA position full penetration high power laser beam welding of up to 30 mm thick AlMg3 plates using electromagnetic weld pool support," *Science and technology of welding and joining*, vol. 17, pp. 128-133, 2012
- [2] Ö. Üstündağ, S. Gook, A. Gumenyuk, and M. Rethmeier, "Hybrid laser arc welding of thick high-strength pipeline steels of grade X120 with adapted heat input," *Journal of Materials Processing Technology*, vol. 275, p. 116358, 2020
- [3] V. Muthupandi, P. Bala Srinivasan, V. Shankar, S. K. Seshadri, and S. Sundaresan, "Effect of nickel and nitrogen addition on the microstructure and mechanical properties of power beam processed duplex stainless steel (UNS 31803) weld metals," *Materials Letters*, vol. 59, pp. 2305-2309, 2005
- [4] A. Karl, "Laserauftragschweißen hochlegierter Duplexstähle," Dissertation, Universität Ilmenau, Ilmenau, 2014
- [5] S. Gook, A. Gumenyuk, and M. Rethmeier, "Hybrid laser arc welding of X80 and X120 steel grade," *Science and technology of welding and joining*, vol. 19, pp. 15-24, 2014
- [6] M. Rethmeier, Gook, S. and Gumenyuk, A., "Einsatz des Laserstrahl-MSG-Hybridschweißverfahrens an längsnahtgeschweißten Großrohren der Güte API-X80/ -X100 zur Steigerung der Zähigkeit und Erhöhung der Wirtschaftlichkeit," Schlussbericht zum Forschungsvorhaben P822 / IGF-Nr. 16415 N2013
- [7] H. C. Wu, L. W. Tsay, and C. Chen, "Laser Beam Welding of 2205 Duplex Stainless Steel with Metal Powder Additions," *ISIJ International*, vol. 44, pp. 1720-1726, 2004
- [8] A. StraÙe, A. Gumenyuk, and M. Rethmeier, "Quality improvement of laser welds on thick duplex plates by laser clad buttering " in *LiM 2019 - Lasers in manufacturing conference 2019, Munich*, pp. 1-6, 2019
- [9] W. S. Pellini, "Strain theory of hot tearing," *Foundry*, vol. 80, pp. 99-125, 1952
- [10] N. N. Prokhorov, "Resistance to hot tearing of cast metals during solidification," *Russian castings production*, vol. 2, pp. 172-175, 1962
- [11] M. Rappaz, J. M. Drezet, and M. Gremaud, "A new hot-tearing criterion," *Metallurgical and Materials Transactions A*, vol. 30, pp. 449-455, 1999
- [12] Z. Yang, X. Zhao, W. Tao, and C. Jin, "Effects of keyhole status on melt flow and flow-induced porosity formation during double-sided laser welding of AA6056/AA6156 aluminium alloy T-joint," *Optics & Laser Technology*, vol. 109, pp. 39-48, 2019
- [13] Masumoto, Tamaki, K., Kutsuna, M., "Hot cracking of austenitic stainless steel weld metal," *Transaction of Japan Welding Society*:1306-1314, 1972
- [14] <https://www.ipgphotonics.com/en/577/Widget/Application+Note+%2311%3A+High+Power+Welding+with+Fiber+Lasers+.pdf>, Last access: 12.03.2020
- [15] M. Sokolov and A. Salminen, "Experimental Investigation of the Influence of Edge Morphology in High Power Fiber Laser Welding," *Physics Procedia*, vol. 39, pp. 33-42, 2012